



Prognostic value of the International Metabolic Prognostic Index for lymphoma patients receiving chimeric antigen receptor T-cell therapy

Michael Winkelmann¹ · Viktoria Blumenberg^{2,3,4} · Kai Rejeski^{2,3,4} · Veit L. Bücklein^{2,3,4} · Michael Ruzicka⁴ · Marcus Unterrainer¹ · Christian Schmidt⁴ · Franziska J. Dekorsy⁵ · Peter Bartenstein^{5,6} · Jens Ricke^{1,6} · Michael von Bergwelt-Baildon^{4,6} · Marion Subklewe^{2,3,4} · Wolfgang G. Kunz^{1,6}

Received: 29 September 2022 / Accepted: 4 December 2022 / Published online: 14 December 2022
© The Author(s), under exclusive licence to Springer-Verlag GmbH Germany, part of Springer Nature 2022

Abstract

Purpose Chimeric antigen receptor T-cell therapy (CART) prolongs survival for patients with relapsed/refractory B-cell non-Hodgkin's lymphoma. The recently introduced International Metabolic Prognostic Index (IMPI) was shown to improve prognostication in the first-line treatment of large B-cell lymphoma. Here, we investigate the prognostic value of the IMPI for progression-free (PFS) and overall survival (OS) in the setting of CD19 CART.

Methods Consecutively treated patients with baseline ¹⁸F-FDG PET/CT imaging and follow-up imaging at 30 days after CART were included. IMPI is composed of age, stage, and metabolic tumor volume (MTV) at baseline and was compared with the International Prognostic Index (IPI). Both indices were grouped into quartiles, as previously described for IPI. In addition, the continuous IMPI was subdivided into tertiles for better separation of risk groups. Overall response rate (ORR), depth of response (DoR), and PFS were determined based on Lugano criteria. Proportional Cox regression analysis studied association of IMPI and IPI with PFS and OS.

Results Thirty-nine patients were included. The IPI was 1 in 23%, 2 in 21%, 3 in 26%, 4 in 21%, and 5 in 10% of the patients. IMPI^{low risk}, IMPI^{intermediate risk}, and IMPI^{high risk} patients had 30-day ORR of 69%, 62%, and 62% and 30-day DoR of –67%, –66%, and –54% with a PFS of 187 days, 97 days, and 87 days, respectively. ORR and DoR showed no correlation with lower IMPI ($r=0.065$, $p=0.697$). Dividing patients into three risk groups showed a significant trend for PFS stratification ($p=0.030$), while IPI did not ($p=0.133$). Neither IPI nor IMPI yielded a significant association with OS after CART (both $p>0.05$).

Conclusion In the context of CART, the IMPI yielded prognostic value regarding PFS estimation. In contrast with IMPI in the first-line DLBCL setting, we did not observe a significant association of IMPI at baseline with OS after CART.

Keywords CAR T-cell therapy · IPI · IMPI · ¹⁸F-FDG PET/CT

This article is part of the Topical Collection on Hematology.

✉ Wolfgang G. Kunz
wolfgang.kunz@med.lmu.de

¹ Department of Radiology, University Hospital, LMU Munich, Marchioninstr. 15, 81377 Munich, Germany

² Laboratory for Translational Cancer Immunology, Gene Center of the LMU Munich, Munich, Germany

³ German Cancer Consortium (DKTK) and Bavarian Center for Cancer Research (BZKF), Partner Site Munich, Munich, Germany

⁴ Department of Medicine III, University Hospital, LMU Munich, Munich, Germany

⁵ Department of Nuclear Medicine, University Hospital, LMU Munich, Munich, Germany

⁶ Comprehensive Cancer Center München-LMU (CCCMLMU), LMU Munich, Munich, Germany

Introduction

Chimeric antigen receptor T-cell therapy (CART) directed against the CD19 antigen [1] has demonstrated efficacy in relapsed/refractory (r/r) large B-cell lymphoma (LBCL) [2–4], follicular lymphoma (FL) [3, 4], and mantle cell lymphoma (MCL) [5]. Compared to historical controls, CART has significantly improved progression-free survival (PFS) and overall survival (OS) [6].

The prognosis of LBCL has historically been estimated by the International Prognostic Index (IPI), introduced in 1993, which includes age, performance status, Ann Arbor stage, serum lactate dehydrogenase (LDH), and extranodal involvement [7]. The IPI score has been shown to be prognostic for PFS in the setting of CART [8, 9], yet no association with OS has been observed [9]. The pivotal trials JULIET and ZUMA-1 showed trends for higher overall response rates (ORR) with lower IPI scores [3, 4], as well as the recent ZUMA-12 trial [10].

The metabolic tumor volume (MTV) of the lymphomas on baseline ^{18}F -Fluorodeoxyglucose positron emission tomography–computed tomography (^{18}F -FDG PET/CT) is prognostic in Hodgkin [11] and several lymphoma subtypes of non-Hodgkin lymphoma including transformed FL [12], MCL [13], and LBCL [14]. Imaging-based response assessment for determination of PFS in most lymphoma entities has most frequently relied on ^{18}F -FDG PET/CT. In current and ongoing phase III trials, the most widely adopted response criteria are based on the Lugano criteria from 2014 [15, 16]. The prognostic value of MTV as a component of a prognostic index has been studied recently using five published trials on DLBCL [17, 18]. The recently introduced International Metabolic Prognostic Index (IMPI) was developed after review of the prognostic potential of the IPI components as well as MTV and resulted in a simplified modification. IMPI only includes age, Ann Arbor stage, and MTV, yet outperformed IPI in survival estimation in the first-line DLBCL treatment setting [17].

We aimed to compare the prognostic value of the IMPI and the historically established IPI for progression-free (PFS) and overall survival (OS) in the context of CD19 CART for r/r B-NHL.

Methods

Study design and population

The study population was based on a prospective registry of all patients consecutively treated with standard-of-care CD19 CART (i.e., axicabtagene ciloleucel,

tisagenlecleucel, brexucabtagene autoleucel) at the Comprehensive Cancer Center Munich of the Ludwig-Maximilian University Munich (CCCM^{LMU}) between January 2019 and May 2022 (data cutoff). The following inclusion criteria were applied:

1. Patients with r/r lymphoma (DLBCL and MCL)
2. Any measurable disease on imaging according to Lugano criteria [15].
3. Available ^{18}F -FDG PET/CT imaging studies at baseline (≤ 2 weeks before CART) and at least at follow-up around 30 days (FU) or before if clinical progression was evident

The following exclusion criteria were applied:

1. Any non-diagnostic imaging studies or missing baseline ^{18}F -FDG PET/CT
2. Patients with non-measurable disease
3. Lack of follow-up examinations or survival data at time of study inclusion

Histologic diagnoses were reviewed by expert pathologists. Patients received lymphodepletion with fludarabine and cyclophosphamide according to the manufacturers' instructions.

Definition of IPI and IMPI

IPI was calculated using age, Eastern Cooperative Oncology Group (ECOG) performance status, Ann Arbor stage, serum LDH, and extranodal involvement [7]. IMPI was calculated using age, Ann Arbor stage, and MTV [17]. Tumor delineations were performed by a board-certified imaging expert. For stratification and statistical analysis, the IPI scores were grouped as 0–1 (low risk), 2 (low intermediate risk), 3 (high intermediate risk), and 4–5 (high risk) as described previously (International Non-Hodgkin's Lymphoma Prognostic Factors Project) [7]. We compared the IMPI with IPI, first dividing the study population into four groups with the same sizes as the IPI categories ($\text{IMPI}^{\text{low risk}}$, $\text{IMPI}^{\text{low intermediate risk}}$, $\text{IMPI}^{\text{high intermediate risk}}$, and $\text{IMPI}^{\text{high risk}}$). For this purpose, we ranked patients to their absolute IMPI and matched patient numbers according with the number of the corresponding IPI risk group. In a second subdivision, the advantage of the interval-scaled IMPI was used to subdivide it into the tertials $\text{IMPI}^{\text{low risk}}$, $\text{IMPI}^{\text{intermediate risk}}$, and $\text{IMPI}^{\text{high risk}}$ to generate 3 groups with the same size for a more detailed breakdown of PFS stratification.

¹⁸F-FDG PET/CT imaging

PET/CT images were acquired approximately 45 min after tracer injection (159–275 MBq weight-adapted with approximately 2.5–4.5 MBq ¹⁸F-FDG per kg bodyweight) and for the FDG PET/CT contrast-enhanced or unenhanced CTs using a slice thickness of 2 mm 120 kVp, 100–400 mAs, and dose modulations were performed for attenuation correction. The following scanners were used: Biograph 64 and Biograph mCT (Siemens Healthineers, Germany) or Discovery 690 (GE Healthcare, USA). Both scanners fulfilled the requirements indicated in the European Association of Nuclear Medicine (EANM) imaging guidelines and obtained EANM Research Ltd. (EARL1) accreditation during acquisition. The following reconstruction algorithms were used: Biograph 64, TrueX (3 iterations, 21 subsets) with Gaussian post-reconstruction smoothing (2 mm full width at half-maximum); Biograph mCT, TrueX (3 iterations, 21 subsets); Discovery 690, VUE Point FX algorithm with 2 iterations and 36 subsets. All systems resulted in a PET image with a voxel size of $2 \times 2 \times 2 \text{ mm}^3$. Images were normalized to decay-corrected injected activity per kg body weight (SUV g/mL).

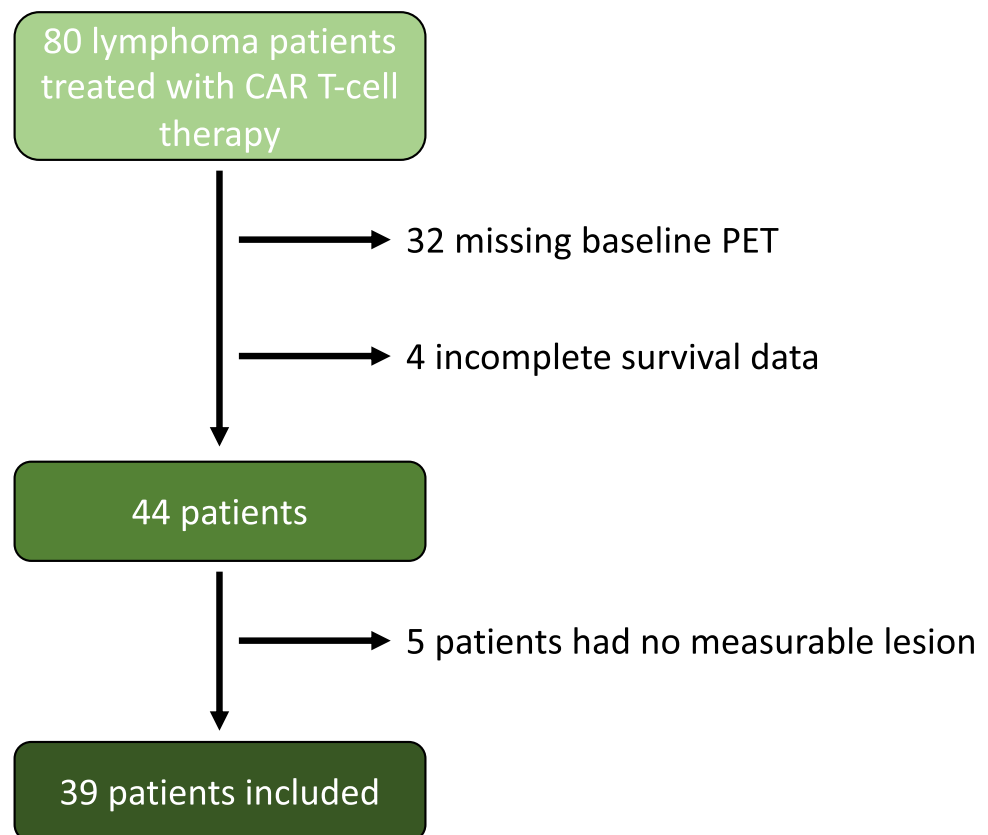
Imaging response assessment

Overall response was determined based on Lugano criteria with segmentation of up to 6 target lesions (TL). The sum of the product of diameters (SPD) was measured to determine tumor burden (TB). DoR was calculated as the percent change of SPD from baseline to 30-day follow-up. Spleen size was measured with splenomegaly being defined by a vertical length $> 13.0 \text{ cm}$. Target lesions (TL), non-target lesions (NTL), and new appearing lesions (NL) during therapy were evaluated quantitatively and qualitatively. All imaging analyses were performed with dedicated trial reporting software mint Lesion 3.8 (mint Medical GmbH; Heidelberg, Germany). The MTV was evaluated using the open-source software platform LIFEx (<https://www.lifexsoft.org>) [19]. Attenuation-corrected PET images were analyzed, and the threshold of the absolute standardized uptake value (SUV) was set to ≥ 4 to define hypermetabolic lymphoma tissue as described before [20, 21].

Statistical analysis

All statistical analyses were performed using GraphPad Prism 9. Proportional Cox regression analysis studied

Fig. 1 Flow chart. A total of 80 lymphoma patients were treated with CAR T-cell therapy at our site. Thirty-two patients did not have a baseline ¹⁸F-FDG PET/CT examination close to the CAR T-cell transfusion, 4 patients were excluded because of lack of survival documentation, and 5 patients did not have a measurable lesion according to the Lugano criteria. Thirty-nine patients met the inclusion criteria



association of IMPI and IPI with PFS and OS. For survival analysis, PFS and OS were visualized using Kaplan–Meier survival curves with categorization for IMPI and IPI as described above. Multivariable regression analysis was used to study associations between IMPI, IPI, and DoR. The overall response rate (ORR) was calculated as the rate of patients with CR and PR. Log-rank (Mantel-Cox) test was performed to examine the significance of the results. p values below 0.05 were considered to indicate statistical significance.

Results

Patient characteristics

Thirty-nine out of 80 patients met the inclusion criteria (median age: 67 years, 38% female). Thirty-two patients had to be excluded because of missing baseline ^{18}F -FDG PET/CT examination close to the CAR-T-cell transfusion, 4 patients were excluded because of lack of survival documentation, and 5 patients did not have a measurable lesion according to the Lugano criteria. A flow chart is provided in Fig. 1. The IPI was determined for all patients. The distribution of IPI scores 1–5 was 23%, 21%, 26%, 21%, and 10%, respectively. Three patients (8%) had stage I disease, 10 patients (26%) stage II, 9 patients (23%) stage III, and 17 patients (44%) stage IV according to Ann Arbor staging system. Twenty-eight out of 39 patients (72%) received a bridging therapy between apheresis and CAR T-cell infusion. Median SPD at baseline was 4835 mm², and median MTV at baseline was 345 mL. Detailed patient characteristics are demonstrated in Table 1.

IMPI and depth of response (DoR)

The DoR as percent increase or decrease in SPD from BL to FU was calculated for all 39 patients and is illustrated in Fig. 2. The color coding of the waterfall plot was chosen according to the categories of the IMPI risk categories. Patients with IMPI^{low risk} were labeled green, with IMPI^{intermediate risk} labeled yellow, and with IMPI^{high risk} labeled red. The majority of patients had a good 30-day DoR, with median percentage change of –67%, –66%, and –54% for IMPI^{low risk}, IMPI^{intermediate risk}, and IMPI^{high risk}, respectively. In 24 of 39 patients (62%), Lugano-based TB decreased by more than 50% 30 days after CART. In 8 patients (21%), there was a slight decrease <50%, and in 1 patient (3%), the size of lymphoma manifestations had not changed. TB increased in 6 patients (15%), by >50% in 4 patients (10%), and by <50% in 2 patients (5%). There was no correlation between DoR, IMPI, and IMPI 3-year PFS ($r=0.065$; $p=0.697$).

Table 1 Patient characteristics

Age	Median	67
Gender	Female:	15 (38%)
	Male:	24 (62%)
Lymphoma entity	LBCL:	31 (79%)
	MCL:	8 (21%)
	- Blastoid MCL	3 (8%)
	- Classic MCL	5 (13%)
Ann Arbor stage	I:	3 (8%)
	II:	10 (26%)
	III:	9 (23%)
	IV:	17 (44%)
IPI	1:	9 (23%)
	2:	8 (21%)
	3:	10 (26%)
	4:	8 (21%)
	5:	4 (10%)
CART Product	Tisagenlecleucel:	19 (49%)
	Axicabtagene ciloleucel:	9 (23%)
	Brexucabtagene autoleucel:	8 (21%)
	Lisocabtagene maraleucel:	3 (8%)
Bridging	Chemotherapy:	22 (56%)
	Immunotherapy:	3 (8%)
	Radiation:	2 (5%)
	Combined therapy:	1 (3%)
	No bridging	11 (28%)
LDH (median)	Apheresis:	377 U/L
	Prior lymphodepletion:	307 U/L
SPD (median)	Total:	4,835 mm ²
	IMPI low risk:	786 mm ²
	IMPI intermediate risk:	7160 mm ²
	IMPI high risk:	10,406 mm ²
MTV (median)	Total:	345 mL
	IMPI low risk:	6 mL
	IMPI intermediate risk:	410 mL
	IMPI high risk:	1199 mL
Probability of 3y-PFS according to IMPI	Total:	77%
	IMPI low risk:	89%
	IMPI intermediate risk:	77%
	IMPI high risk:	62%

CAR chimeric antigen receptor, LBCL large B-cell lymphoma, IMPI International Metabolic Prognostic Index, IPI International Prognostic Index, LDH lactate dehydrogenase, MCL mantle cell lymphoma, MTV metabolic tumor volume, SPD sum of the product diameters

Imaging-based overall response

Overall response rate (ORR) was similar for all IMPI risk categories. IMPI^{low risk}, IMPI^{intermediate risk}, and IMPI^{high risk} patients had a 30-day ORR of 69%, 62%, and 62%, respectively. Imaging-based response classification of the different IMPI risk groups by Lugano criteria also showed only

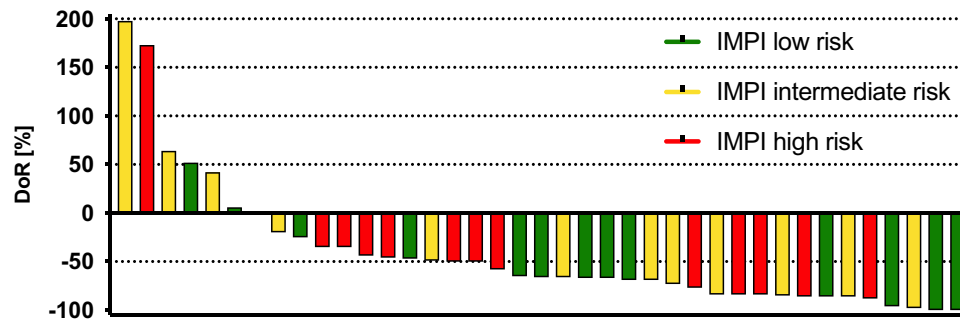


Fig. 2 Depth of response and IMPI. Color-coded waterfall plot for depth of response (DoR) as percentage change of Lugano tumor burden (TB) of all patients from baseline to follow-up 30 days after

CART. Positive values indicate an increase and negative values a decrease in TB. Bars are labeled red for IMPI^{high risk}, yellow for IMPI^{intermediate risk}, and green for IMPI^{low risk} at baseline

Table 2 Influence of IMPI on imaging endpoints at 90 days and on PFS

	ORR	DoR	PFS	CR	PR	SD	PD
IMPI ^{low risk}	69%	-508.9 mm ² (-67%)	187 d	3 (23%)	6 (46%)	2 (15%)	2 (15%)
IMPI ^{intermediate risk}	62%	-2,881.2 mm ² (-66%)	97 d	2 (15%)	6 (46%)	1 (8%)	4 (31%)
IMPI ^{high risk}	62%	-6,543.7 mm ² (-54%)	87 d	1 (8%)	7 (54%)	4 (31%)	1 (8%)

Comparison of different risk groups (low, intermediate, and high) based on tertiles of the International Metabolic Prognostic Index (IMPI). Shown are overall response rates (ORR) and depth of response (DoR) as change in sum of the product diameters (SPD) of up to 6 target lesions from baseline to follow-up 30 days after CART. In addition, median PFS, number of patients with complete response (CR, green), partial response (PR, yellow), stable disease (SD, gray), and progressive disease (PD, red) as defined by Lugano criteria are displayed

minor differences. In the IMPI^{low risk} group, 3 patients (23%) showed CR, 6 patients (46%) PR, 2 patients (15%) SD, and 2 patients (15%) PD at 30-day FU. Of the 13 IMPI^{intermediate risk} patients, 2 patients (15%) had CR, 6 patients (46%) PR, 1 patient (8%) SD, and 4 patients (31%) PD. In the IMPI^{high risk} group, 1 patient (8%) was detected with CR, 7 patients (54%) with PR, 4 patients (31%) with SD, and 1 patient (8%) with PD.

IPI and IMPI scores and imaging endpoints

For the same three IMPI-based risk groups, we performed an analysis of association with PFS. The median Lugano-based PFS was 187 days, 97 days, and 87 days for IMPI^{low risk}, IMPI^{intermediate risk}, and IMPI^{high risk} patients, respectively (Table 2). A moderate negative correlation between IMPI 3y-PFS probability and IPI ($r = -0.672$, $p < 0.001$) and a moderate positive correlation between PFS and OS ($r = 0.619$, $p < 0.001$) was observed. IPI and the size-adjusted IMPI groups were not able to stratify PFS (both $p > 0.05$). However, dividing patients into three risk groups IMPI^{low risk}, IMPI^{intermediate risk}, and IMPI^{high risk} according to their IMPI 3y-PFS probability showed a significant trend for

PFS stratification ($p = 0.030$). Neither IPI nor IMPI yielded a significant association with OS after CART (both $p > 0.05$). Kaplan–Meier curves for PFS and OS with the different group forms are depicted in Fig. 3A–C.

Discussion

In our study set in the context of later-line CART for r/r B-NHL patients, the IMPI outperformed the IPI for prognostication of PFS. However, we did not find a significant association with ORR, DoR, and OS, neither for IMPI nor for IPI, in this patient population. Unlike first-line LBCL treatment, the prognostic relevance of IMPI (and possibly IPI) regarding OS may therefore be limited in the CART setting.

In the first-line treatment setting, the association of imaging endpoint surrogates of survival such as PFS with OS has been established [22, 23]. In contrast, later disease stages may reflect phenotypic and metabolic changes of the lymphoma manifestations themselves, which may in turn affect these associations [24, 25]. Typically, more widespread nodal locations are involved, and extranodal lesions are more

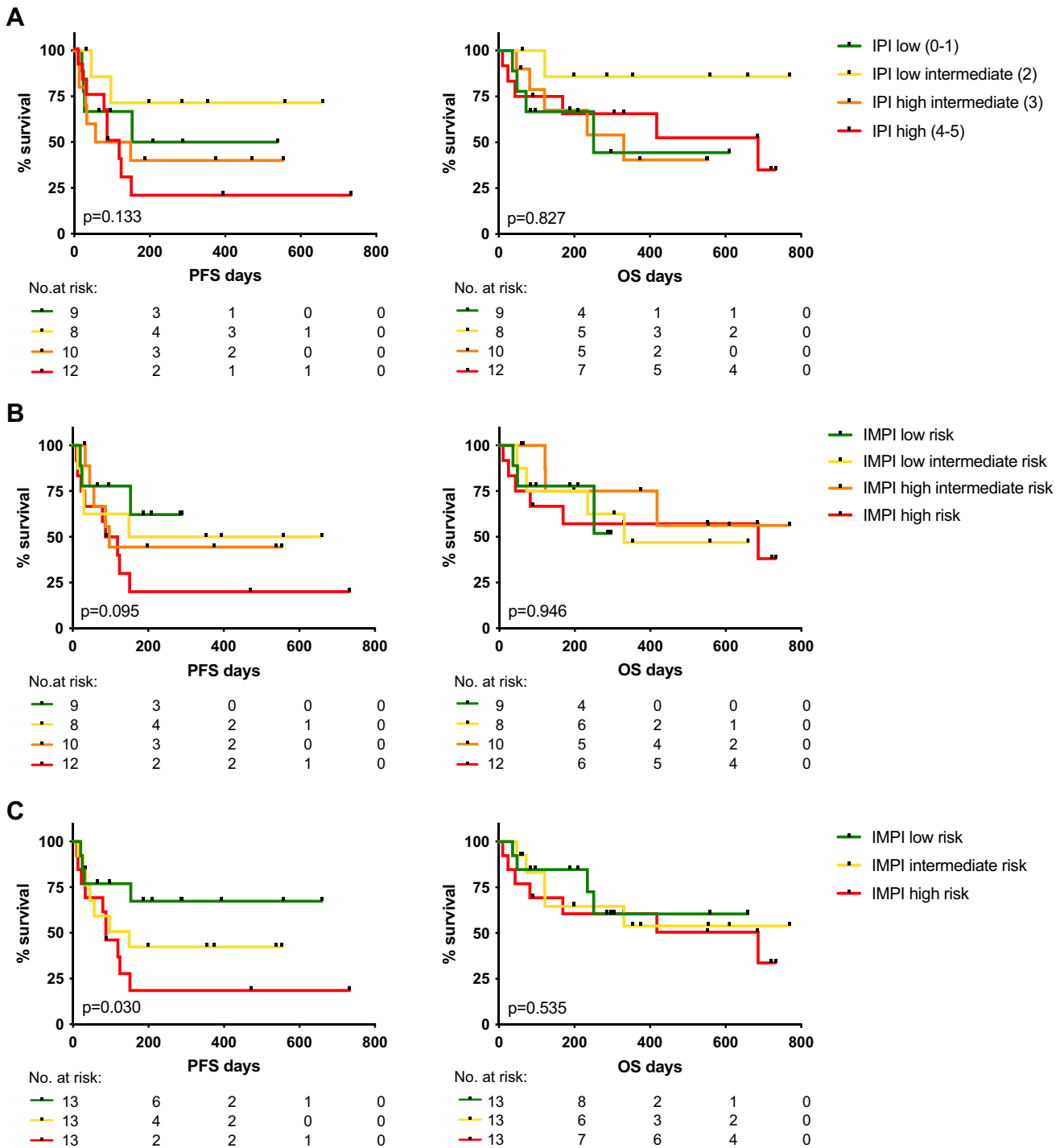


Fig. 3 Survival Stratification by IPI and IMPI. Depicted are the Kaplan–Meier curves for progression-free survival (PFS, left) and overall survival (OS, right). The upper row (A) shows the color-coded Kaplan–Meier curves according to the IPI groups with low risk (IPI 0–1, green), low intermediate risk (IPI 2, yellow), high intermediate risk (IPI 3, orange), and high risk (IPI 4–5, red). The middle row (B)

demonstrates the survival curves for the size-adjusted IMPI groups analogous to the IPI groups with the same color coding. The lower row (C) depicts a split of the IMPI groups by tertiles into 3 equally sized groups with the following color coding: IMPI low risk (green), IMPI intermediate risk (yellow), and IMPI high risk (red)

frequently encountered. Importantly, these imaging findings are associated with elevated systemic inflammatory markers, which are of prognostic interest in the context of CART

[26–28]. Notably, prognostic indices have so far not been adapted to such changes in the disease course, and data on association with OS is scarce [15, 29].

In our study population, the division of groups according to the originally published 4 risk groups [7] was not able to stratify PFS or OS. This could be due to the limited number of subjects in this study. Another explanation is that the IPI might have a different prognostic value in context of later line treatments such as CART. Consistent with this would be that division of patients into a low-risk IPI group (IPI 0–2) and a high-risk group (IPI 3–5) showed a small non-significant difference in PFS in our cohort (Supplemental Fig. 1A) but no difference in OS (Supplemental Fig. 1B), as previously published in the setting of CART [9].

Novel prognostic indices, imaging endpoints, and response criteria in lymphoma will likely evolve from selected lesion-based assessments (as, e.g., with the Lugano criteria) to whole tumor burden quantification (as, e.g., with MTV). In the first-line setting, the IMPI has outperformed the conventional IPI in estimating outcome of DLBCL patients. Notably, MTV has replaced the three components LDH, Ann Arbor stage, and performance status [17]. This indicates that whole tumor burden may contain more important prognostic information and that other less granular clinical or serological data may carry some redundant information.

To our knowledge, there is no literature comparing IMPI and IPI in the context of advanced lymphoma under CAR T-cell therapy. Our study has limitations which need to be considered when interpreting the results. First, this is a single-center study with a limited number of subjects. This may limit the interpretation of the association of IMPI or IPI with OS. Second, some patients had to be excluded as there was no measurable disease on PET. This represents a limitation of imaging-based prognostic indices (as compared with IPI) in clinical routine. Third, resulting from the operational and logistical nature of CART, the clinical use of bridging therapy may affect the MTV as the metabolic activity is likely altered by systemic bridging regimens. During the bridging period, this may affect the metabolic component of the lymphomas more strongly than the morphologic lymphoma masses, which could also affect the prediction of OS.

In conclusion, the IMPI yielded superior prognostic value compared to the IPI alone regarding the estimation of PFS following CD19 CART and thus holds potential as a novel prognostic index. In contrast with IMPI in the first-line DLBCL setting, we did not observe a significant association of IMPI at baseline with OS after CART. Future research should prospectively assess the value of IMPI regarding OS in larger studies of r/r B-NHL patients receiving CART.

Supplementary Information The online version contains supplementary material available at <https://doi.org/10.1007/s00259-022-06075-2>.

Author contribution M.W. and W.G.K. conceived and design the study; V.B., K.R., V.L.B., M.R., M.U., and C.S. collected the data; M.W., V.B., K.R., V.L.B., and W.G.K. analyzed and interpreted the data; and

M.W. and W.G.K. drafted the manuscript; and V.B., K.R., F.J.D., P.B., J.R., M.v.B.-B., and M.S. revised the manuscript.

Funding The work was supported by funding from the research program “Förderung für Forschung und Lehre (FöFoLe) project number 1147” of the Medical Faculty of Ludwig Maximilian University (LMU) Munich and the Bavarian Cancer Research Center (BZKF) to M.W. The work was further supported by the Else-Kröner-Fresenius Stiftung (to V.B.) and the German Cancer Consortium DKTK (to V.B.).

Data availability The datasets generated during and/or analyzed during the current study are available from the corresponding author on reasonable request.

Declarations

Ethics approval All medical records and imaging studies were reviewed with the approval of the LMU Munich Institutional Review Board (LMU Ethics Committee, project number 19–817).

Consent to participate Informed consent was obtained from all individual participants included in the study.

Competing interests V.B. has received industry research support from Gilead, Novartis, Celgene, and Roche. K.R. declares having received research funding and travel support from Kite/Gilead and honoraria from Novartis. C.S. received travel support from Kite/Gilead. M.v.B.-B. received research funding and honoraria from Novartis, Kite Pharma, Miltenyi Biotec, Mologen, MSD, Astellas, and Roche. M.S. received industry research support from Amgen, Gilead, Miltenyi Biotec, MorphoSys, Roche, and Seattle Genetics; served as a consultant or advisor to Amgen, Bristol Myers Squibb, Celgene, Gilead, Pfizer, Novartis, and Roche; is on the advisory boards of Amgen, Celgene, Gilead, Janssen, Novartis, Pfizer, and Seattle Genetics; and serves on the speaker’s bureau at Amgen, Celgene, Gilead, Janssen, and Pfizer. The remaining authors declare no competing financial interests.

References

1. June CH, Sadelain M. Chimeric antigen receptor therapy. *N Engl J Med*. 2018;379:64–73. <https://doi.org/10.1056/NEJMra1706169>.
2. Schuster SJ, Bishop MR, Tam CS, Waller EK, Borchmann P, McGuirk JP, Jager U, Jaglowski S, Andreadis C, Westin JR, et al. Tisagenlecleucel in adult relapsed or refractory diffuse large B-cell lymphoma. *N Engl J Med*. 2019;380:45–56. <https://doi.org/10.1056/NEJMoa1804980>.
3. Schuster SJ, Svoboda J, Chong EA, Nasta SD, Mato AR, Anak O, Brogdon JL, Pruteanu-Malinici I, Bhoj V, Landsburg D, et al. Chimeric antigen receptor T cells in refractory B-cell lymphomas. *N Engl J Med*. 2017;377:2545–54. <https://doi.org/10.1056/NEJMoa1708566>.
4. Neelapu SS, Locke FL, Bartlett NL, Lekakis LJ, Miklos DB, Jacobson CA, Braunschweig I, Oluwole OO, Siddiqi T, Lin Y, et al. Axicabtagene ciloleucel CAR T-cell therapy in refractory large B-cell lymphoma. *N Engl J Med*. 2017;377:2531–44. <https://doi.org/10.1056/NEJMoa1707447>.
5. Wang M, Munoz J, Goy A, Locke FL, Jacobson CA, Hill BT, Timmerman JM, Holmes H, Jaglowski S, Flinn IW, et al. KTE-X19 CAR T-cell therapy in relapsed or refractory mantle-cell lymphoma. *N Engl J Med*. 2020;382:1331–42. <https://doi.org/10.1056/NEJMoa1914347>.
6. Ghione P, Palomba ML, Patel AR, Bobillo S, Deighton K, Jacobson CA, Nahas M, Hatswell AJ, Jung AS, Kanters S, et al. Comparative

- effectiveness of ZUMA-5 (axi-cel) vs SCHOLAR-5 external control in relapsed/refractory follicular lymphoma. *Blood*. 2022;140:851–60. <https://doi.org/10.1182/blood.2021014375>.
7. International Non-Hodgkin's Lymphoma Prognostic Factors P. A predictive model for aggressive non-Hodgkin's lymphoma. *N Engl J Med*. 1993;329:987–94. <https://doi.org/10.1056/NEJM199309303291402>.
 8. Bethge WA, Martus P, Schmitt M, Holtick U, Subklewe M, von Tresckow B, Ayuk F, Wagner-Drouet EM, Wulf GG, Marks R, et al. GLA/DRST real-world outcome analysis of CAR-T cell therapies for large B-cell lymphoma in Germany. *Blood*. 2022. <https://doi.org/10.1182/blood.2021015209>.
 9. Garcia-Recio M, Wudhikarn K, Pennisi M, Alonso-Trillo R, Flynn J, Shouval R, Afuye AO, Silverberg ML, Batlevi CW, Dahi P, et al. The International Prognostic Index is associated with outcomes in diffuse large B cell lymphoma after chimeric antigen receptor T cell therapy. *Transplant Cell Ther*. 2021;27:233–40. <https://doi.org/10.1016/j.jct.2020.10.022>.
 10. Neelapu SS, Dickinson M, Munoz J, Ulrickson ML, Thieblemont C, Oluwole OO, Herrera AF, Ujjani CS, Lin Y, Riedell PA, et al. Axicabtagene ciloleucel as first-line therapy in high-risk large B-cell lymphoma: the phase 2 ZUMA-12 trial. *Nat Med*. 2022. <https://doi.org/10.1038/s41591-022-01731-4>.
 11. Cottreau AS, Versari A, Loft A, Casasnovas O, Bellei M, Ricci R, Bardet S, Castagnoli A, Brice P, Raemaekers J, et al. Prognostic value of baseline metabolic tumor volume in early-stage Hodgkin lymphoma in the standard arm of the H10 trial. *Blood*. 2018;131:1456–63. <https://doi.org/10.1182/blood-2017-07-795476>.
 12. Meignan M, Cottreau AS, Versari A, Chartier L, Dupuis J, Boussetta S, Grassi I, Casasnovas RO, Haioun C, Tilly H, et al. Baseline metabolic tumor volume predicts outcome in high-tumor-burden follicular lymphoma: a pooled analysis of three multicenter studies. *J Clin Oncol*. 2016;34:3618–26. <https://doi.org/10.1200/JCO.2016.66.9440>.
 13. Albano D, Bosio G, Bianchetti N, Pagani C, Re A, Tucci A, Giubbini R, Bertagna F. Prognostic role of baseline 18F-FDG PET/CT metabolic parameters in mantle cell lymphoma. *Ann Nucl Med*. 2019;33:449–58. <https://doi.org/10.1007/s12149-019-01354-9>.
 14. Ceriani L, Gritti G, Cascione L, Piroso MC, Polino A, Ruberto T, Stathis A, Bruno A, Moccia AA, Giovannella L, et al. SAKK38/07 study: integration of baseline metabolic heterogeneity and metabolic tumor volume in DLBCL prognostic model. *Blood Adv*. 2020;4:1082–92. <https://doi.org/10.1182/bloodadvances.201901201>.
 15. Cheson BD, Fisher RI, Barrington SF, Cavalli F, Schwartz LH, Zucca E, Lister TA, Alliance AL, Lymphoma G, Eastern Cooperative Oncology G, et al. Recommendations for initial evaluation, staging, and response assessment of Hodgkin and non-Hodgkin lymphoma: the Lugano classification. *J Clin Oncol*. 2014;32:3059–68. <https://doi.org/10.1200/JCO.2013.54.8800>.
 16. Barrington SF, Mikhael NG, Kostakoglu L, Meignan M, Hutchings M, Mueller SP, Schwartz LH, Zucca E, Fisher RI, Trotman J, et al. Role of imaging in the staging and response assessment of lymphoma: consensus of the International Conference on Malignant Lymphomas Imaging Working Group. *J Clin Oncol*. 2014;32:3048–58. <https://doi.org/10.1200/JCO.2013.53.5229>.
 17. Mikhael NG, Heymans MW, Eertink JJ, de Vet HCW, Boellaard R, Duhren U, Ceriani L, Schmitz C, Wieggers SE, Huttman A, et al. Proposed new dynamic prognostic index for diffuse large B-cell lymphoma: International Metabolic Prognostic Index. *J Clin Oncol*. 2022. <https://doi.org/10.1200/JCO.21.02063>. (JCO2102063).
 18. Vercellino L. High total metabolic tumor volume at baseline predicts survival independent of response to therapy. *Blood*. 2020;135(16):1396–405.
 19. Nioche C, Orhac F, Boughdad S, Reuze S, Goya-Outi J, Robert C, Pellot-Barakat C, Soussan M, Frouin F, Buvat I. LIFEX: a free-ware for radiomic feature calculation in multimodality imaging to accelerate advances in the characterization of tumor heterogeneity. *Cancer Res*. 2018;78:4786–9. <https://doi.org/10.1158/0008-5472.CAN-18-0125>.
 20. Tutino F, Puccini G, Linguanti F, Puccini B, Rigacci L, Kovalchuk S, Sciagra R, Berti V. Baseline metabolic tumor volume calculation using different SUV thresholding methods in Hodgkin lymphoma patients: interobserver agreement and reproducibility across software platforms. *Nucl Med Commun*. 2021;42:284–91. <https://doi.org/10.1097/MNM.0000000000001324>.
 21. Martin-Saladich Q, Reyes-Llompert G, Sabate-Llobera A, Palomar-Munoz A, Domingo-Domenech E, Cortes-Romera M. Comparison of different automatic methods for the delineation of the total metabolic tumor volume in I-II stage Hodgkin Lymphoma. *Sci Rep*. 2020;10:12590. <https://doi.org/10.1038/s41598-020-69577-9>.
 22. Batlevi CL, Younes A. Surrogate end points in lymphoma. *Ann Oncol*. 2018;29:1622–3. <https://doi.org/10.1093/annonc/mdy219>.
 23. Zhu J, Yang Y, Tao J, Wang SL, Chen B, Dai JR, Hu C, Qi SN, Li YX. Association of progression-free or event-free survival with overall survival in diffuse large B-cell lymphoma after immunochemotherapy: a systematic review. *Leuk Off J Leuk Soc Am Leuk Res Fund UK*. 2020;34:2576–91. <https://doi.org/10.1038/s41375-020-0963-1>.
 24. Adams HJ, de Klerk JM, Fijnheer R, Heggelman BG, Dubois SV, Nievelstein RA, Kwee TC. Where does diffuse large B-cell lymphoma relapse? *J Comput Assist Tomogr*. 2016;40:531–6. <https://doi.org/10.1097/RCT.0000000000000395>.
 25. Figura NB, Robinson TJ, Sim AJ, Wang X, Cao B, Chavez JC, Shah BD, Khimani F, Lazaryan A, Davila M, et al. Patterns and predictors of failure in recurrent or refractory large B-cell lymphomas after chimeric antigen receptor T-cell therapy. *Int J Radiat Oncol Biol Phys*. 2021. <https://doi.org/10.1016/j.ijrobp.2021.06.038>.
 26. Rejeski K, Perez A, Iacoboni G, Penack O, Bucklein V, Jentzsch L, Mouggiakakos D, Johnson G, Arciola B, Carpio C, et al. The CAR-HEMATOTOX risk-stratifies patients for severe infections and disease progression after CD19 CAR-T in R/R LBCL. *J Immunother Cancer*. 2022. <https://doi.org/10.1136/jitc-2021-004475>.
 27. Rejeski K, Perez A, Sesques P, Hoster E, Berger C, Jentzsch L, Mouggiakakos D, Frolich L, Ackermann J, Bucklein V, et al. CAR-HEMATOTOX: a model for CAR T-cell-related hematologic toxicity in relapsed/refractory large B-cell lymphoma. *Blood*. 2021;138:2499–513. <https://doi.org/10.1182/blood.2020010543>.
 28. Jain MD, Zhao H, Wang X, Atkins R, Menges M, Reid K, Spittler K, Faramand R, Bachmeier C, Dean EA, et al. Tumor interferon signaling and suppressive myeloid cells are associated with CAR T-cell failure in large B-cell lymphoma. *Blood*. 2021;137:2621–33. <https://doi.org/10.1182/blood.2020007445>.
 29. Eisenhauer EA, Therasse P, Bogaerts J, Schwartz LH, Sargent D, Ford R, Dancey J, Arbuck S, Gwyther S, Mooney M, et al. New response evaluation criteria in solid tumours: revised RECIST guideline (version 1.1). *Eur J Cancer*. 2009;45:228–47. <https://doi.org/10.1016/j.ejca.2008.10.026>.

Publisher's note Springer Nature remains neutral with regard to jurisdictional claims in published maps and institutional affiliations.

Springer Nature or its licensor (e.g. a society or other partner) holds exclusive rights to this article under a publishing agreement with the author(s) or other rightsholder(s); author self-archiving of the accepted manuscript version of this article is solely governed by the terms of such publishing agreement and applicable law.